

# INORGANIC CHEMISTRY

## FRONTIERS





## RESEARCH ARTICLE



Cite this: *Inorg. Chem. Front.*, 2016, **3**, 1058

## Nanoparticles of chitosan conjugated to organo-ruthenium complexes†

Yanqing Wang,<sup>a,b</sup> Anaís Pitto-Barry,<sup>b</sup> Abraha Habtemariam,<sup>b</sup> Isolda Romero-Canelon,<sup>b</sup> Peter J. Sadler<sup>\*b</sup> and Nicolas P. E. Barry<sup>\*b</sup>

The synthesis of nanoparticles of conjugates of caffeic acid-modified chitosan with ruthenium arene complexes is described. The chemical structure and physical properties of the nanoparticles were characterised by electronic absorption spectroscopy (UV-vis), Fourier transform infrared spectroscopy (FT-IR), <sup>1</sup>H NMR spectroscopy, dynamic light scattering (DLS), transmission electron microscopy (TEM), X-ray powder diffraction (XRD), and circular dichroism (CD) analysis. The multi-spectral results revealed that caffeic acid is covalently bound to chitosan and chelates to {Ru(*p*-cymene)Cl}<sup>+</sup>. The DLS studies indicated that the Ru-caffeic acid modified chitosan nanoparticles are well-defined and of nanometre size. Such well-defined nanocomposites of chitosan and metal complexes might find a range of applications, for example in drug delivery.

Received 4th May 2016,  
Accepted 11th June 2016

DOI: 10.1039/c6qi00115g

rs.c.li/frontiers-inorganic

### Introduction to the international collaboration

Yanqing Wang from Yancheng Teachers University, People's Republic of China is developing a research programme in the exciting area of medicinal inorganic chemistry, and in particular the design of nanoparticles for the delivery of metal anticancer complexes. He was awarded a research fellowship from the Jiangsu Overseas Research & Training Program for University Prominent Young & Middle-aged Teachers and President to spend the year from February 2014 to February 2015 in the laboratory of Peter Sadler at the University of Warwick, UK. There he carried out research in bioinorganic chemistry on topics related to the design and synthesis of nanoparticle conjugates of natural polymers with organo-ruthenium complexes. He synthesised nanocomposites of caffeic acid-modified chitosan linked to ruthenium arene complexes. Chitosan is deacetylated chitin, found in the exoskeleton of crustaceans and cell walls of fungi. Such well-defined nanocomposites of chitosan and metal complexes might find a range of applications, for example in drug delivery.

## Introduction

Nanocarriers are constituted of sub-micron particles (≤100 nm) with various morphologies such as nanocapsules, polymer nanoparticles, liposomes, micelles.<sup>1</sup> The innovation in such systems lies in the fact that they eliminate a number of impediments that hamper the action of conventional drugs.<sup>2</sup> The solubility of poorly water soluble drugs may be controlled by entrapping them into crystalline nano suspensions,<sup>3</sup> or by combination with organic or lipid nanoparticles to ensure their circulation in blood for longer periods of time.<sup>4</sup> Nanoparticles (NPs) made of polymers are of particular interest as drug delivery systems, owing to their synthetic versatility, as well as their tuneable properties (*e.g.* thermosensitivity and

pH-response).<sup>5–7</sup> Examples of metallated NPs include micellar metal-based MRI or SPECT/CT imaging agents,<sup>8,9</sup> and formulation NC-6004 or Nanoplatin™ (cisplatin encapsulated in micelles composed of PEG and poly(γ-benzyl-L-glutamate) (PEG-PGlu)), which is under phase I/II clinical evaluation for the treatment of pancreatic cancer.<sup>10</sup>

The development of nanostructured materials functionalised with metal complexes as alternatives for administering anticancer metallodrugs is currently receiving attention with synthetic polymers,<sup>11–20</sup> however, little is known about the utilisation of natural polymers. Nanoparticles based on biopolymers, such as the cationic polysaccharide chitosan, have been demonstrated to possess various favourable features including those for drug and gene delivery, biosensing, therapy, and molecular imaging because of their excellent high biocompatibility, bio-degradation, hydrophilicity, and low toxicity toward mammalian cells.<sup>21–24</sup> The hydroxyl and amine groups located on the backbone of chitosan allow simple chemical modifications (*e.g.* *via* Schiff-bases and metal chelation), thus enabling the design of libraries of multifunctional structures of chitosan with potential for biological applications.<sup>25</sup>

<sup>a</sup>Institute of Applied Chemistry and Environmental Engineering, Yancheng Teachers University, Yancheng City, Jiangsu Province 224002, People's Republic of China

<sup>b</sup>Department of Chemistry, University of Warwick, Gibbet Hill, Coventry, CV4 7AL, UK. E-mail: N.Barry@warwick.ac.uk, P.J.Sadler@warwick.ac.uk

†Electronic supplementary information (ESI) available. See DOI: 10.1039/c6qi00115g



Here we report the synthesis of novel nano-construct materials made up of ruthenium complexes with biocompatible and biodegradable chitosan macro-ligands, thereby opening the way to chitosan controlled metallodrug delivery. Modifications of the  $\text{NH}_2$  functional group in the chitosan matrix provide a platform for the introduction of the capability to interact strongly with ruthenium(II) ions through complex formation. Caffeic acid was selected to modify chitosan because it is a natural product commonly found in *e.g.* coffee, olive oil, white wine, and cabbage<sup>26</sup> and acts as carcinogenic inhibitor and shows antiradical-scavenging activity *in vitro*.<sup>27</sup> The complexes formed involving caffeic acid-modified chitosan and a Ru(II) arene are characterised by UV-vis, FT-IR, circular dichroism (CD), TEM, XRD, and NMR measurements.

## Materials and methods

### Materials

Chitosan, caffeic acid, 1-ethyl-3(3-dimethylaminopropyl) carbodiimide hydrochloride (EDC), and *N*-hydroxysuccinimide (NHS) were purchased from Sigma-Aldrich.  $\text{RuCl}_3 \cdot 3\text{H}_2\text{O}$  was purchased from Precious Metals Online (PMO Pty Ltd). The *p*-cymene Ru dimer was prepared as described in the literature.<sup>28</sup> Anhydrous quality of ethanol, tetrahydrofuran and dichloromethane were used (Aldrich). All other chemicals were analytical grade, and used as received.

### Synthesis

Chitosan (1.0 g) was dissolved at 1% (w/v) in acetic acid (100 mL), followed by dilution with methanol (80 mL) under stirring at ambient temperature. The required amount of caffeic acid per sugar residue of chitosan (0.5 mol/mol) was dissolved in methanol and was added to the chitosan solution. Then equal amounts (1.5 mol equiv./[caffeic acid]) of EDC and NHS were added into the polymer solution, which allowed the formation of amide linkages by the reaction with primary amino groups in chitosan. The resulting reaction mixture was stirred for 24 hours at ambient temperature, dialysed for 3 days against excess water/methanol mixture (v/v 1/4), and lyophilised to obtain a white powder of caffeic acid-modified chitosan.<sup>29</sup> For Ru loading, 100 mg of the template-free mesoporous polymer was dispersed in 20 mL of  $\text{H}_2\text{O}$  in a round-bottom flask. To this was added 20 mg (or 50 mg) dichlorido(*p*-cymene)ruthenium dimer (ruthenium dimer) dispersed in  $\text{CH}_3\text{OH}$  (20 mL), then the mixture was stirred vigorously for 24 h. The resulting solution was dialysed for 3 days against an excess amount of water/methanol (4/1 v/v) to obtain caffeic acid-modified chitosan–ruthenium nanoparticles.

### Characterisation methods

UV-vis and UV-vis-near IR spectra were recorded on Cary 400 UV-vis and PE Lambda 950 spectrophotometers, respectively. FT-IR spectra were obtained on a Nicolet 6700 spectrometer

(Thermo Company). X-ray diffraction (XRD) patterns were obtained on a D8ADVANCE (Bruker) diffractometer with  $\text{Cu K}\alpha$  radiation ( $\lambda = 0.154 \text{ nm}$ ). CD spectra were recorded with a Jasco J-810 spectropolarimeter, using a quartz cell with a path length of 1 cm.  $^1\text{H}$  NMR spectra of samples were recorded on a Bruker ARX 400 spectrometer using deuterated solvents. Chemical shifts are reported as  $\delta$  in parts per million using the residual protiated solvent as internal standard. The polymer sample was dissolved in a  $\text{CD}_3\text{COOD}/\text{D}_2\text{O}$  (1% v/v) solution to a concentration of  $20 \text{ mg mL}^{-1}$ . Caffeic acid (5 mM) was dissolved in  $\text{CD}_3\text{OD}$ . Transmission electron microscopy images were obtained using a JEOL 2000FX microscope operating at 200 keV. The samples were prepared at ambient temperature by placing a drop (5  $\mu\text{L}$ ) on a Quantifoil R2/2 TEM grid. The hydrodynamic diameter of nanoparticles was determined by dynamic light scattering (DLS) using a Malvern Zetasizer NanoS instrument operating at 25 °C with a 4 mW He–Ne 633 nm laser module. Measurements were made at a detection angle of 173° (back scattering) and the data were analysed using Malvern DTS 6.20 software. The hydrodynamic radius was calculated from the Stokes–Einstein equation where particles are assumed to be spherical.

## Results and discussion

The synthesis of nanostructured materials made of ruthenium arene complexes with biocompatible and biodegradable chitosan macro-ligands followed a two-step process (Scheme 1). Caffeic acid-modified chitosan was first synthesised *via* amidation reactions, before being reacted with the *para*-cymene ruthenium dimer  $[(\eta^6\text{-}p\text{-cym})\text{Ru}(\mu\text{-Cl})\text{Cl}]_2$ , to give the metalated particles made of biodegradable, natural polymers (Scheme 1).

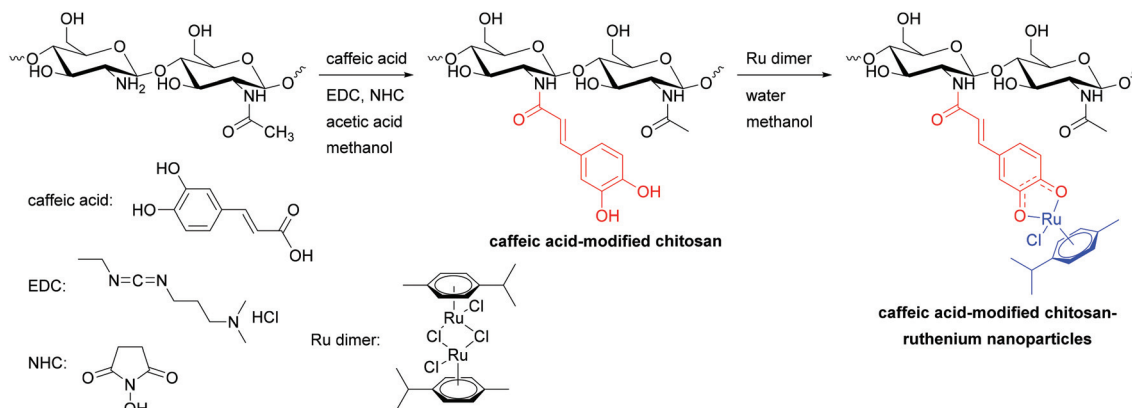
### Caffeic acid-modified chitosan

**Synthesis.** Caffeic acid and chitosan were reacted with EDC and NHS in a methanol solution to form amide linkages. The resulting reaction mixture was stirred for 24 hours at ambient temperature, dialysed for 3 days against excess water/methanol mixture (v/v 1/4), and lyophilised to obtain a white powder of caffeic acid-modified chitosan.

**UV-vis spectroscopy.** The UV spectra of chitosan, caffeic acid and chitosan-caffeic acid are shown in Fig. 1. Caffeic acid-modified chitosan (blue line) has two main absorption peaks at 285 and 320 nm, assigned to  $n\text{-}\pi^*$  transition from  $\text{-OH}$  to the aromatic ring and a  $\pi\text{-}\pi^*$  transition of the aromatic ring. The above results indicated that caffeic acid has modified the chitosan units. Based on the absorption spectra, the grafting ratio of caffeic acid on chitosan was found to be 5.7% [caffeic acid in sample (mg)/sample (mg)].

**$^1\text{H}$  NMR spectroscopy.**  $^1\text{H}$  NMR spectra of chitosan, caffeic acid, chitosan-caffeic acid are shown in Fig. 2. Chitosan has a resonance at 2.0 ppm corresponding to the methyl protons of the acetylated glucosamine residues, peaks between 3.3 and





**Scheme 1** Synthetic route for caffeic acid-modified chitosan–ruthenium nanoparticles.

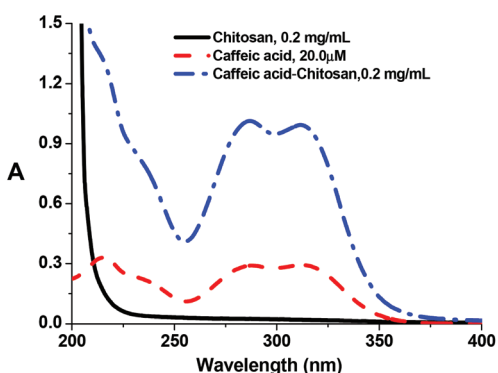


**Fig. 1** UV spectra of chitosan ( $0.2 \text{ mg mL}^{-1}$ ), caffeic acid ( $20 \mu\text{M}$ ), chitosan-caffeic acid ( $0.2 \text{ mg mL}^{-1}$ ) in  $18 \text{ m}\Omega \text{ cm}$  water,  $T = 298 \text{ K}$ .

4.5 ppm assignable to the protons of C-3, C-4, C-5, and C-6 of the pyranose ring, and peaks at 3.1 and 4.8 ppm corresponding to C-2 and C-5 protons of the glucosamine residues.<sup>30</sup> In the case of the caffeic acid-modified chitosan, new peaks assignable to caffeic acid are observed, which confirms the conjugation of caffeic acid to the chitosan backbone.

**FT-IR spectroscopy.** The FT-IR spectra of chitosan and chitosan-caffeic acid are illustrated in Fig. 3. The FT-IR spectrum of chitosan shows large and intense bands at  $3366 \text{ cm}^{-1}$  corresponding to the hydrogen-bonded O–H stretches overlapped with several N–H stretching bands.<sup>31</sup> The characteristic absorption bands at  $1657$ ,  $1561$  and  $1317 \text{ cm}^{-1}$  are assignable to C=O stretching (amide I), N–H bending (amide II) and C–N stretching (amide III) modes of the residual *N*-acetyl groups, respectively.<sup>32</sup> Chitosan-caffeic acid showed decreases in intensity of bands associated with protonated glucosamine residues of chitosan at  $1420$  and  $1457 \text{ cm}^{-1}$ , indicating a loss of  $-\text{NH}_3^+$  groups and formation of covalent links between the phenol groups of caffeic acid and the amino groups of chitosan.<sup>33,34</sup>

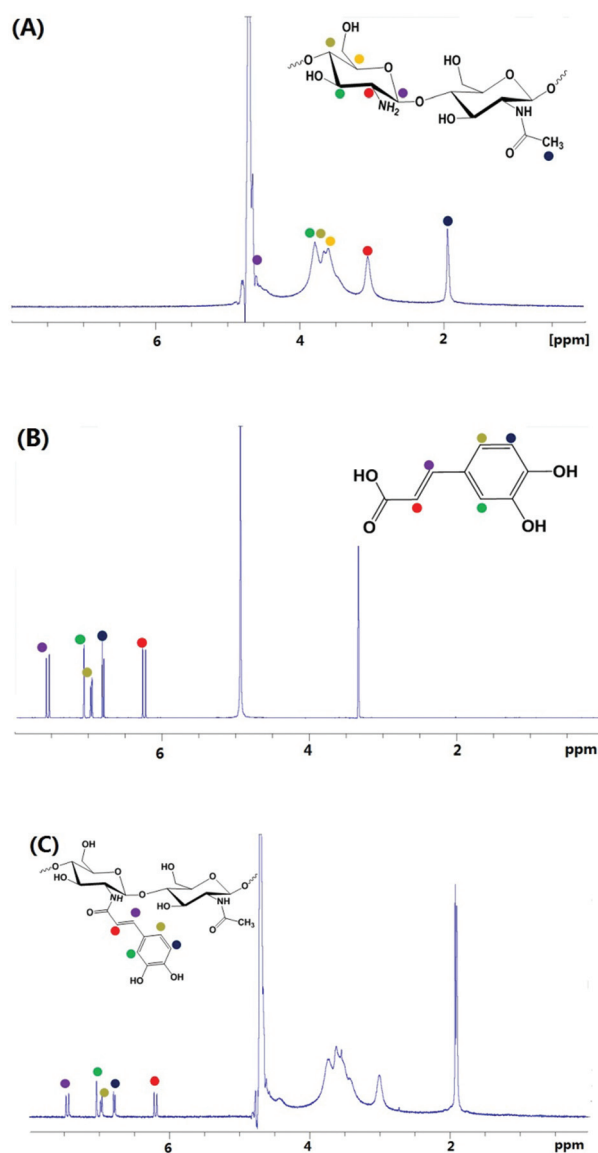


**Fig. 2**  $^1\text{H}$  NMR spectra of (A) chitosan in  $1\% \text{ CD}_3\text{COOD}$  in  $\text{D}_2\text{O}$ , (B) caffeic acid in  $\text{CD}_3\text{OD}$ , and (C) chitosan-caffeic acid in  $\text{D}_2\text{O}$ .



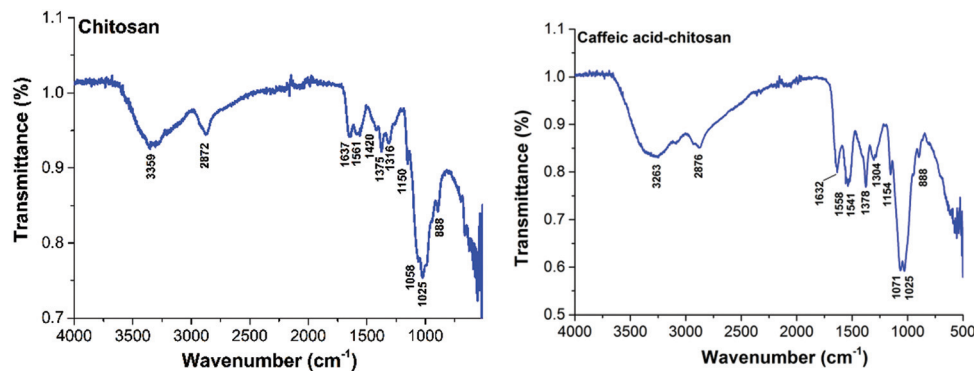


Fig. 3 FT-IR spectra of chitosan and chitosan-caffeic acid.

### Ruthenium-caffeic acid modified chitosan complex

**Synthesis.** Caffeic acid-modified chitosan-ruthenium nanoparticles were synthesised by reaction of dichlorido(*p*-cymene) ruthenium dimer with a H<sub>2</sub>O solution of template-free mesoporous polymer in a weight ratio 1:2 (or 1:5), followed by 3 days dialysis against an excess amount of water/methanol (Scheme 1 and Materials and methods).

**UV-vis spectrometry.** The UV-vis spectra of Ru dimer, caffeic acid-modified chitosan and Ru-caffeic acid-modified chitosan are presented in Fig. 4.

The absorption bands of the Ru-caffeic acid-modified chitosan compound (blue line) at *ca.* 885 nm can be assigned to ligand-to-Ru(II) charge transfer.<sup>35</sup> The intensity of the two main bands at *ca.* 285 and 312 nm decreased remarkably after ligation of ruthenium to the caffeic acid catechol group. These confirm the formation of a complex between ruthenium and caffeic acid-modified chitosan *via* the binding of the Ru(II) centre and the two oxygen atoms from the catechol unit. Fig. 5 shows the kinetic profile of the reaction between the caffeic acid-modified chitosan and the ruthenium dimer by UV-visible spectroscopy. A bathochromic shift of the absorption



Fig. 5 The UV-vis spectra for the reaction of Ru dimer with caffeic acid-modified chitosan at different reaction times, [Ru dimer] =  $2.0 \times 10^{-5}$  mol L<sup>-1</sup>, [caffeic acid in caffeic acid-modified chitosan] =  $4.0 \times 10^{-5}$  mol L<sup>-1</sup>, in water.

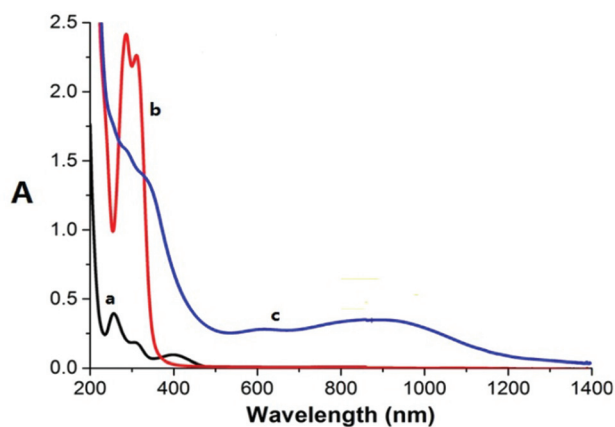


Fig. 4 The UV-vis spectra of Ru dimer (a), caffeic acid-modified chitosan (b) and Ru-caffeic acid-modified chitosan (c), [Ru dimer] =  $1.5 \times 10^{-4}$  mol L<sup>-1</sup>, [caffeic acid-chitosan] = 0.4 mg mL<sup>-1</sup>, in water.

band from *ca.* 312 nm to *ca.* 319 nm is observed after addition of the ruthenium dimer. The shift increases with time up to a value of *ca.* 331 nm after 1 h. This confirms the formation of the complex between the ruthenium and the caffeic acid-modified chitosan. Moreover, such a value is obtained after a few minutes, which indicates that the reaction progresses quickly.

Fig. 6 shows UV-vis spectra for the reaction of the Ru dimer with caffeic acid-modified chitosan at different initial concentrations of Ru dimer. The UV-vis absorption bands at *ca.* 285 nm and 312 nm decreased with increasing concentration of the Ru dimer and isosbestic points are observed at 267 and 325 nm. When the value of [Ru]/[caffeic acid] reaches 1, the intensity of the absorption bands reaches a maximum value. These results indicate that a 1:1 complex is formed between [(*p*-cymene)RuCl]<sup>-1</sup> and caffeic acid on chitosan and that interactions occur between ruthenium and caffeic acid on the chitosan.

**Dynamic light scattering studies.** Dynamic light scattering was used to determine the size of the particles of Ru-caffeic



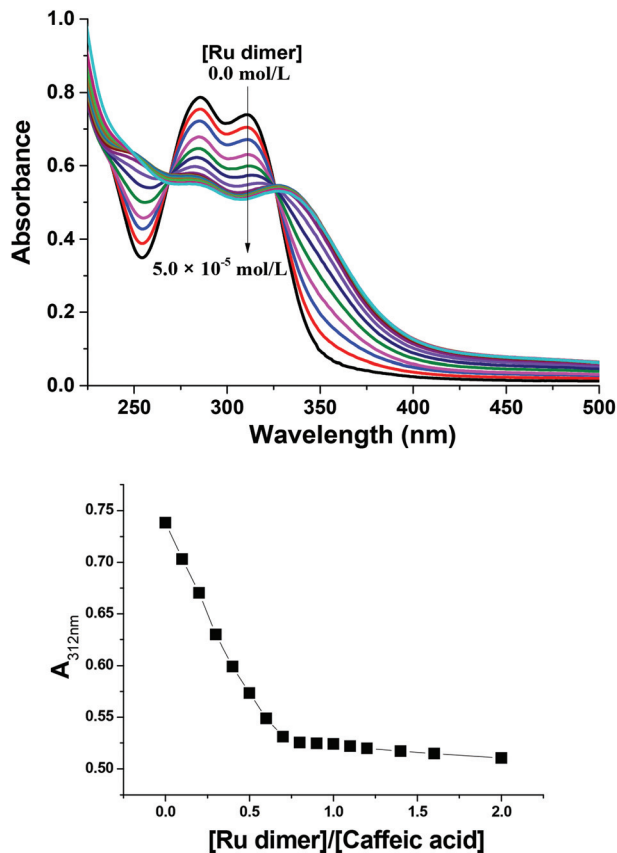


**Fig. 6** Top: UV-vis spectra for the reaction of various concentrations of Ru dimer with caffeic acid-modified chitosan, [caffeic acid in caffeic acid-modified chitosan] =  $5.0 \times 10^{-5} \text{ mol L}^{-1}$ , in water. Bottom: Changes in absorbance at 312 nm at various concentrations of Ru dimer with caffeic acid-modified chitosan.

acid-modified chitosan. Fig. 7 shows that the hydrodynamic diameter for the Ru-caffeic acid-modified chitosan with different ratios of [caffeic acid]/[Ru dimer] ranges from 30 to

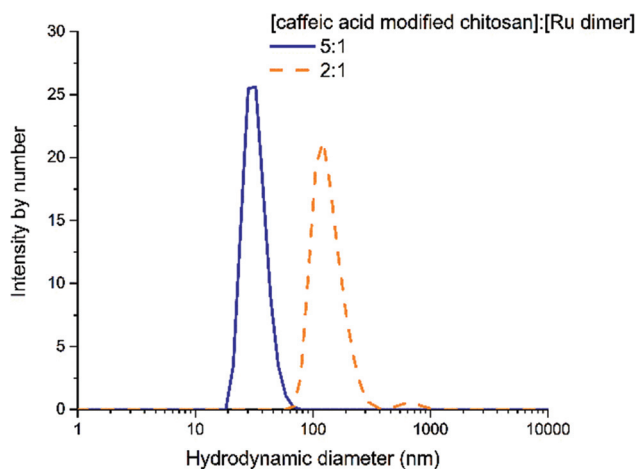


**Fig. 7** Dynamic light scattering of Ru-caffeic acid modified chitosan at two different ratios. Spectra were recorded at 25 °C;  $2 \text{ mg mL}^{-1}$ ; the solutions were not filtered before analysis.

120 nm. Interestingly, only one population of particles is found per loading degree, suggesting that the interactions between the ruthenium ions and the polymer backbone are controllable in terms of the architectures obtained.

**Transmission electron microscopy.** Dry-state TEM samples were prepared after dialysis of the particles for 4 days but a drying effect was observed which led to a spreading of the chitosan nanoparticles (see Fig. S1†). No information regarding the size of the particles can thus be retrieved from the dry-state TEM. However, the noticeable difference in contrast between the metallic parts of the particles (shown by arrows in Fig. S1†) and the organic parts of the polymer chains, shows that the ruthenium ions did not dissociate from the caffeic acid-modified chitosan after dialysis, suggesting a relatively strong bonding between the metal and its ligands (in accordance with the proposed chelated structure).

**Powder X-ray diffractometry of Ru-caffeic acid-modified chitosan.** The X-ray diffractograms of chitosan, caffeic acid-modified chitosan, and Ru-caffeic acid-modified chitosan are presented in Fig. 8. It was observed that the diffractogram of chitosan consisted of two major peaks at *ca.*  $10.0^\circ$  and  $20.1^\circ$ . Compared with chitosan, the diffractogram of caffeic acid-modified chitosan exhibited some changes in peak intensity and peak width. The peak at  $10.0^\circ$  disappeared, while the peak intensity at around  $20.1^\circ$  decreased and the peak width increased. Such a weaker and broader peak indicated a more amorphous phase of the caffeic acid-modified chitosan matrix. In addition, the peak at *ca.*  $20.1^\circ$  of Ru-caffeic acid-modified chitosan disappeared, implying that the Ru-caffeic acid-modified chitosan was considerably more amorphous than chitosan and caffeic acid-modified chitosan. The structure of chitosan was greatly perturbed by anchoring ruthenium complexes to its backbone.

**CD spectroscopy of Ru-caffeic acid modified chitosan.** The circular dichroism spectra of caffeic acid-modified chitosan solution in the absence and presence of Ru dimer are shown in Fig. 9. The CD spectrum of caffeic acid-modified chitosan

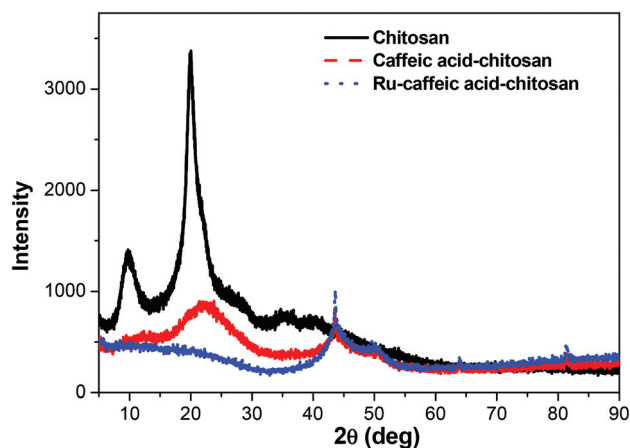


**Fig. 8** XRD of chitosan, caffeic acid-modified chitosan, and Ru-caffeic acid-modified chitosan.



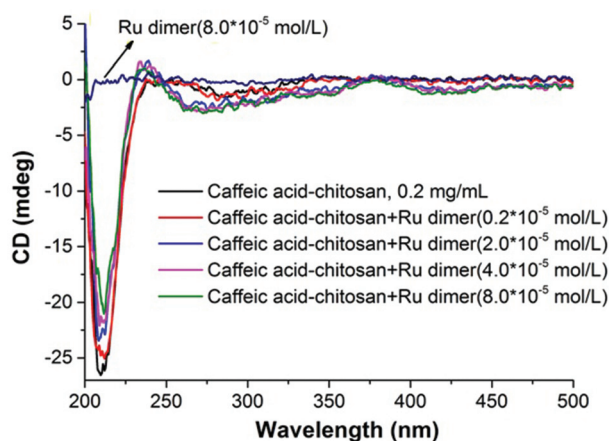


Fig. 9 CD spectra of caffeic acid modified chitosan in the absence and presence of Ru dimer.

in the absence of Ru dimer exhibits a strong negative CD band at *ca.* 210 nm, which corresponds to  $n \rightarrow \pi^*$  electronic transitions of the  $-\text{NH}-\text{CO}-$  chromophore of GlcNAc units. The Ru dimer did not show circular dichroism bands at 210 nm. As shown in Fig. 9, the intensity of the main CD band of caffeic acid-modified chitosan is higher than that of the caffeic acid-chitosan modified by interacting with the Ru dimer, which suggests that Ru binding induces a change of molecular forces, symmetry, and backbone structure of chitosan. In addition, the CD band at about 285 nm shifted to 270 nm, which indicates the formation of a complex between ruthenium and caffeic acid-modified chitosan.

## Conclusions

Nanoparticles of chitosan bearing anchored ruthenium complexes *ca.* 20 nm in size were prepared and studied by UV-vis, FT-IR, NMR, DLS, TEM, XRD, and CD analysis. The multi-spectral results reveal that strong interactions are present between ruthenium and the oxygen atoms of the catechol unit on caffeic acid. The analysis of the particles in aqueous solution by dynamic light scattering revealed the nanometric size of the Ru-caffeic acid-modified chitosan nanoparticles. In addition, reaction with the Ru dimer appears to induce a change of molecular forces, symmetry, and backbone structure of chitosan. These results suggest that the Ru-caffeic acid modified chitosan nanoparticles have potential for investigation as alternative polymer-based metal anticancer drugs. Furthermore, (*O,O*)-chelated ligands in anticancer complexes of the type  $[\text{Ru}(\eta^6\text{-arene})(\text{O},\text{O}\text{-chelate})\text{Cl}]^{2+}$  have been shown not only to be labile in solution (formation of the hydroxo-bridged dimer  $[(\eta^6\text{-arene})\text{Ru}_2(\mu\text{-OH})_3]^+$ ),<sup>36</sup> but also to increase the rate and extent of hydrolysis,<sup>37</sup> suggesting that the ruthenium unit should readily be released from the chitosan nanoparticles.

## Acknowledgements

We thank the National Natural Science Foundation of China (Project No. 21571154), the Jiangsu Overseas Research & Training Program for University Prominent Young & Middle-aged Teachers and Presidents, Leverhulme Trust (Early Career Fellowship No. ECF-2013-414 to NPEB), the ERC (Grant No. 247450 to PJS), EPSRC (EP/F034210/1 to PJS) and Science City (AWM/ERDF) for support, and EU COST Action CM1105 for stimulating discussions.

## References

- H. S. Oberoi, N. V. Nukolova, A. V. Kabanov and T. K. Bronich, *Adv. Drug Delivery Rev.*, 2013, **65**, 1667–1685.
- J. K. Vasir, M. K. Reddy and V. Labhsetwar, *Curr. Nanosci.*, 2005, **1**, 47–64.
- B. E. Rabinow, *Nat. Rev. Drug Discovery*, 2004, **3**, 785–796.
- W. A. Wani, S. Prashar, S. Shreaz and S. Gómez-Ruiz, *Coord. Chem. Rev.*, 2016, **312**, 67–98.
- R. Gref, Y. Minamitake, M. T. Peracchia, V. Trubetsky, V. Torchilin and R. Langer, *Science*, 1994, **263**, 1600–1603.
- J. V. Jokerst, T. Lobovkina, R. N. Zare and S. S. Gambhir, *Nanomedicine*, 2011, **6**, 715–728.
- N. Kamaly, Z. Xiao, P. M. Valencia, A. F. Radovic-Moreno and O. C. Farokhzad, *Chem. Soc. Rev.*, 2012, **41**, 2971–3010.
- K. J. Haxton and H. M. Burt, *J. Pharm. Sci.*, 2009, **98**, 2299–2316.
- B. Hoang, H. Lee, R. M. Reilly and C. Allen, *Mol. Pharmaceutics*, 2009, **6**, 581–592.
- N. P. E. Barry and P. J. Sadler, *ACS Nano*, 2013, **7**, 5654–5659.
- A. Valente, M. H. Garcia, F. Marques, Y. Miao, C. Rousseau and P. Zinck, *J. Inorg. Biochem.*, 2013, **127**, 79–81.
- K. Kaur, M. Kaur, A. Kaur, J. Singh, N. Singh, S. K. Mittal and N. Kaur, *Inorg. Chem. Front.*, 2014, **1**, 99–108.
- Q. Cheng, H. Shi, H. Huang, Z. Cao, J. Wang and Y. Liu, *Chem. Commun.*, 2015, **51**, 17536–17539.
- R. Plummer, R. H. Wilson, H. Calvert, A. V. Boddy, M. Griffin, J. Sludden, M. J. Tilby, M. Eatock, D. G. Pearson, C. J. Ottley, Y. Matsumura, K. Kataoka and T. Nishiya, *Br. J. Cancer*, 2011, **104**, 593–598.
- H. Chen, W. He and Z. Guo, *Chem. Commun.*, 2014, **50**, 9714–9717.
- N. P. E. Barry, A. Pitto-Barry, I. Romero-Canelon, J. Tran, J. J. Soldevila-Barreda, I. Hands-Portman, C. J. Smith, N. Kirby, A. P. Dove, R. K. O'Reilly and P. J. Sadler, *Faraday Discuss.*, 2014, **175**, 229–240.
- M. Callari, J. R. Aldrich-Wright, P. L. de Souza and M. H. Stenzel, *Prog. Polym. Sci.*, 2014, **39**, 1614–1643.
- G. Zhou, I. I. Harruna and C. W. Ingram, *Polymer*, 2005, **46**, 10672–10677.
- E. M. Linares, A. Formiga, L. T. Kubota, F. Galembeck and S. Thalhammer, *J. Mater. Chem. B*, 2013, **1**, 2236–2244.



- 20 A. Anitha, S. Sowmya, P. T. S. Kumar, S. Deepthi, K. P. Chennazhi, H. Ehrlich, M. Tsurkan and R. Jayakumar, *Prog. Polym. Sci.*, 2014, **39**, 1644–1667.
- 21 M. S. Verma, S. Liu, Y. Y. Chen, A. Meerasa and F. X. Gu, *Nano Res.*, 2011, **5**, 49–61.
- 22 Y. Yang, S.-X. Yuan, L.-H. Zhao, C. Wang, J.-S. Ni, Z.-G. Wang, C. Lin, M.-C. Wu and W.-P. Zhou, *Mol. Pharm.*, 2015, **12**, 644–652.
- 23 F. S. Majedi, M. M. Hasani-Sadrabadi, J. J. VanDersarl, N. Mokarram, S. Hojjati-Emami, E. Dashtimoghadam, S. Bonakdar, M. A. Shokrgozar, A. Bertsch and P. Renaud, *Adv. Funct. Mater.*, 2014, **24**, 418–418.
- 24 P. Agrawal, G. J. Strijkers and K. Nicolay, *Adv. Drug Delivery Rev.*, 2010, **62**, 42–58.
- 25 H. Zhu, F. Liu, J. Guo, J. Xue, Z. Qian and Y. Gu, *Carbohydr. Polym.*, 2011, **86**, 1118–1129.
- 26 A. O. Aytakin, S. Morimura and K. Kida, *J. Biosci. Bioeng.*, 2011, **111**, 212–216.
- 27 J. H. Chen and C.-T. Ho, *J. Agric. Food Chem.*, 1997, **45**, 2374–2378.
- 28 J. Tönnemann, J. Risse, Z. Grote, R. Scopelliti and K. Severin, *Eur. J. Inorg. Chem.*, 2013, **2013**, 4558–4562.
- 29 S. Kwon, J. H. Park, H. Chung, I. C. Kwon, S. Y. Jeong and I.-S. Kim, *Langmuir*, 2003, **19**, 10188–10193.
- 30 D.-S. Lee, J.-Y. Woo, C.-B. Ahn and J.-Y. Je, *Food Chem.*, 2014, **148**, 97–104.
- 31 G. He, X. Chen, Y. Yin, H. Zheng, X. Xiong and Y. Du, *Carbohydr. Polym.*, 2011, **83**, 1274–1278.
- 32 J. Liu, X.-Y. Wen, J.-F. Lu, J. Kan and C.-H. Jin, *Int. J. Biol. Macromol.*, 2014, **65**, 97–106.
- 33 J. C. Shiu, M.-H. Ho, S.-H. Yu, A.-C. Chao, Y.-R. Su, W.-J. Chen, Z.-C. Chiang and W. P. Yang, *Carbohydr. Polym.*, 2010, **79**, 724–730.
- 34 A. Aljawish, I. Chevalot, B. Piffaut, C. Rondeau-Mouro, M. Girardin, J. Jasniewski, J. Scher and L. Muniglia, *Carbohydr. Polym.*, 2012, **87**, 537–544.
- 35 F. Hasanain and Z. Y. Wang, *Dyes Pigm.*, 2009, **83**, 95–101.
- 36 M. Melchart, A. Habtemariam, S. Parsons, S. A. Moggach and P. J. Sadler, *Inorg. Chim. Acta*, 2006, **359**, 3020–3028.
- 37 R. Fernández, M. Melchart, A. Habtemariam, S. Parsons and P. J. Sadler, *Chem. – Eur. J.*, 2004, **10**, 5173–5179.

